Proceedings of the ASME 2024
International Design Engineering Technical Conferences and
Computers and Information in Engineering Conference
IDETC/CIE2024
August 25-28, 2024, Washington, DC

IDETC2024-143517

A DISASSEMBLY SCORE FOR HUMAN-ROBOT COLLABORATION CONSIDERING ROBOTS' CAPABILITIES

Hao-Yu Liao

Environmental Engineering Sciences University of Florida, Gainesville, FL, 32611 <u>haoyuliao@ufl.edu</u>

Jef R. Peeters

Department of Mechanical Engineering, KU Leuven, Flanders Make@KU Leuven, Leuven, Belgium jef.peeters@kuleuven.be

ABSTRACT

Product disassembly is essential for remanufacturing operations and recovery of end-of-use devices. However, disassembly has often been performed manually with significant safety issues for human workers. Recently, human-robot collaboration has become popular to reduce the human workload and handle hazardous materials. However, due to the current limitations of robots, they are not fully capable of performing every disassembly task. It is critical to determine whether a robot can accomplish a specific disassembly task. This study develops a disassembly score which represents how easy is to disassemble a component by robots, considering the attributes of the component along with the robotic capability. Five factors, including component weight, shape, size, accessibility, and positioning, are considered when developing the disassembly score. Further, the relationship between the five factors and robotic capabilities, such as grabbing and placing, is discussed. The MaxViT (Multi-Axis Vision Transformer) model is used to determine component sizes through image processing of the XPS 8700 desktop, demonstrating the potential for automating disassembly score generation. Moreover, the proposed disassembly score is discussed in terms of determining the appropriate work setting for disassembly operations, under three main categories: human-robot collaboration (HRC), semi-HRC, and worker-only settings. A framework for calculating disassembly time, considering human-robot collaboration, is also proposed.

Keywords: Human-Robot Collaboration, Disassembly Score, Ease of Disassembly, Machine Learning, Automated Rating Systems, Remanufacturing

Terrin Pulikottil

Department of Mechanical Engineering, KU Leuven Flanders Make@KU Leuven, Leuven, Belgium terrin.pulikottil@kuleuven.be

Sara Behdad*

Environmental Engineering Sciences University of Florida, Gainesville, FL, 32611 sarabehdad@ufl.edu

1. INTRODUCTION

Disassembly is necessary to break down used products, such as electronic waste (e-waste) for end-of-use recovery. The increasing rate of e-waste generation creates significant environmental and health risks due to the improper disposal and management of toxic materials in discarded electronics. Disassembly reduces the risk of e-waste by facilitating the extension of the product life cycle through reuse, remanufacture, and recycling. One of the primary challenges for remanufacturers is to make disassembly operations economically viable through strategies such as the use of robots for addressing the labor-intensive nature of disassembly and developing analytical solutions for identifying the best sequence to dismantle a device [1], [2].

The end-of-life phase is often overlooked in product design, and disassembly and recyclability usually do not receive enough attention during the design phase. Previous literature has tried to develop disassemblability score [3] and ease of disassembly metric (eDiM) [4] assuming that disassembly is performed manually. These metrics determine how difficult it is to disassemble a product by human workers. Table 1 summarizes several existing metrics relevant to disassembly. The metrics include repair scores that consider disassembly, such as the iFixit score [5], and the Assessment Matrix for Ease of Repair (AsMeR) [6]; the metrics developed for replacement such as Priority Replacement Index (PRI) [7]; and finally the metrics specifically for disassembly such as eDiM [8] and disassemblability [9]. These scores have a wide range of applications, particularly when evaluating different design alternatives, and design-for-X methods) [10].

Table 1: Examples of relevant disassembly scores.

Methods	References
Repair metrics such as iFixit score, and Assessment Matrix for ease of Repair (AsMeR)	[5], [11]
Replacement metrics such as Priority Replacement Index (PRI)	[12]
Disassembly metrics such as Ease of Disassembly Metric (eDiM), and Disassemblability	[13], [14]

Previous studies have highlighted the importance of considering disassemblability. For example, Qiu et al. (2014) adopted a weighted design structure matrix (DSM) to analyze disassemblability based on product configuration [9]. Germani et al. (2014) evaluated the disassemblability during the product design phase [15]. Zhu et al. (2020) assessed the disassemblability of an entire product rather than components for the product's maintainability [14]. Sawanishi et al. (2015) studied the disassembleability of mobile phones to increase the feasibility of reuse and design improvements [16]. Ali et al. (2022) defined a quantitative evaluation metric for disassembly by considering the returning quality, design features of the product, and technological requirements [17]. Parsa et al. (2019) considered disassembly handling, operation, demand, and cost to evaluate the degree of disassemblability [18]. Go et al. (2011) reviewed the disassemblability of end-of-life vehicles and discussed the relationship between disassembly time and disassembly scores [19]. Rodriguez et al. (2023) addressed the disassemblability and the importance of disassembly for repair [20].

In recent years, human-robot collaboration (HRC) and robotic-assisted disassembly have become popular due to the potential for reducing human fatigue [21] and removing hazardous materials [22]. The disassemblability can determine whether the robot can complete the specific disassembly task or

not [23]. Although previous studies have discussed disassembly scores, the disassemblability score that considers the capabilities of robots is still a research gap. Nonetheless, such a disassembly score would be a practical source for design improvements to assess product circularity and facilitate initiatives such as right-to-repair in Industry 4.0.

This study develops a disassembly score from the robotic aspect. The score determines how easily robots can dismantle a component. Five factors, including component size, shape, weight, accessibility, and positioning, have been considered. The impact of these factors on robotic capabilities, such as grabbing and placing, has been further discussed. Finally, the proper work setting (e.g., HRC, Semi-HRC, and worker only) is decided based on the disassembly score to show how the proposed disassembly score can be used in practice. Moreover, the disassembly time in the aspect of the human worker and the robot is discussed. To automate the process of developing such scores, the MaxViT machine learning model is applied to identify the component size using detailed segmented images.

The remainder of this paper is organized as follows. Section 2 discusses the methodology for developing the proposed disassembly score. Section 3 discusses a case study to demonstrate the application of the proposed disassembly score. Section 4 discusses the results, and Section 5 concludes the paper.

2. METHODOLOGY

This section discusses the process of developing the disassembly score, the factors considered, and a machine learning model to recognize competent size as one of the disassembly factors.

2.1 Disassembly scores

Figure 1 shows the relationship between the five factors, robotic capability, and work settings.

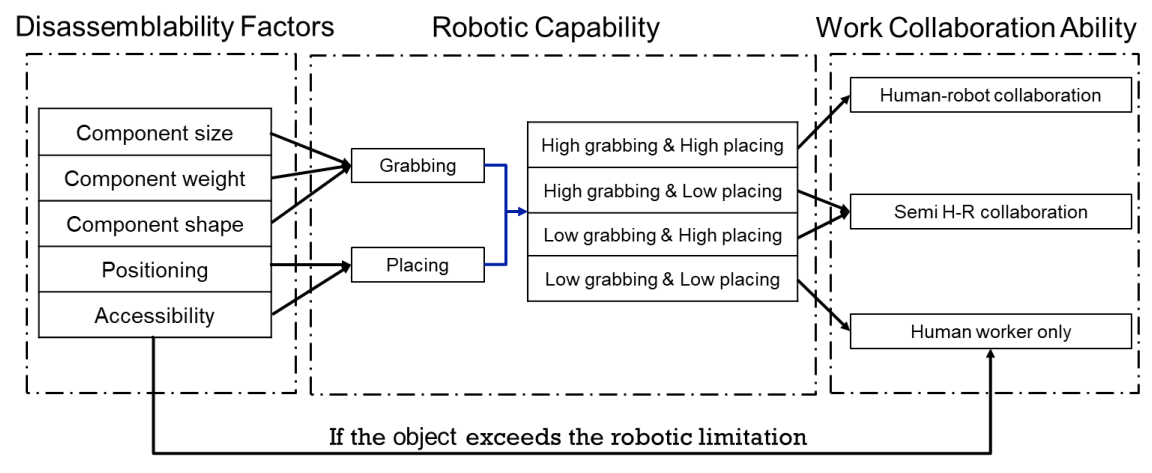


Figure 1: The relationship between disassembly factors, robotic capability, and work settings.

2.1.1 Disassemblability Factors

Table 2 shows the five factors, where each factor has three categories, with the corresponding score for each category ranging from 1, 3, to 5. A higher score means the robot better handles the object. For example, if the component size is small, the score is 1. The component size and component weight depend on the robotic capability. While some robots are designed for heavy lifting, there is an upper limit to the weight they can handle. Also, robots have size constraints. Robots designed for specific tasks may not be able to handle objects significantly larger or smaller than those they are programmed to work with. The size and weight limits are defined based on 33% and 66% of robotic capability.

The component shape is defined by reflective symmetric using the following Equation [24]:

Symmetric value =
$$1 - \frac{A_d}{A_L}$$
 (1)

Upon identifying the axis of symmetry, two regions are evaluated. The larger region donates as A_L , is contrasted with the smaller one to determine the disparity in their areas, represented as A_d . A value of $A_d = 0$ indicates no discrepancy between the two regions, showing that the shape is symmetrical.

Table 2: The disassembly factors, scores, and the corresponding criteria.

Factors	Scores	Criteria
Component	Large (5)	> 56.7 mm & < 85 mm
size	Medium (3)	> 28.3mm & < 56.7 mm
	Small (1)	< 28.3 mm
Component	Light (5)	< 1.67 kg
weight	Medium (3)	> 1.67 kg & < 3.33 kg
	Heavy (1)	3.33 kg & < 5 kg
Component	Symmetric (5)	1
shape	Semi-symmetric	>= 0.5
_	(3)	
	Asymmetric (1)	< 0.5
Positioning	Ease to grasp(5)	Square or
		RS order of 2, 4, 6
	Moderate to	Cycle or RS order is an
	grasp (3)	odd number or greater
		than 6
	Difficult to	The RS order is 1 (no
	grasp (1)	rotational symmetry) and
		no line is parallel
Accessibility	High (5)	Accessible without
		removing any components
	Medium (3)	Accessible by removing
		one component
	Limited (1)	Removing more than two
		obstacles or
		No space for the gripper

The positioning is determined based on the Rotational Symmetry (RS). The categorization of objects based on RS order facilitates their classification in terms of ease of manipulation.

Rotational Symmetry (RS) is known by a shape's ability to maintain symmetry upon being rotated. The degree of rotation required to achieve this symmetry is referred to as the order of RS.[25]. Specifically, objects with an even RS order are considered easy to grasp. On the other hand, objects with an odd RS order, cyclical shapes, or an RS order that exceeds six present moderate difficulty for grabbing. An RS order of one indicates the absence of rotational symmetry and the challenge of robotic handling. Furthermore, accessibility is determined by the number of components that should be removed to access the current component, which depends on the robotic gripper's size. Adequate space is needed so that the robot can quickly grasp the object.

2.1.2 Robotic capability

In this study, the UR5e robot, equipped with a Robotiq gripper, is used to show the application of the proposed disassembly score. The UR5e's specifications, as listed in the manual, include a maximum payload capacity of 5 kg and a gripper opening of up to 8.5 cm. Based on these specifications, disassembly factors such as component size and weight are categorized into two thresholds, 33% and 66% of the robot's capability, as summarized in Table 2. We should note that the criteria for disassembly score can vary with the type of robotic arm used. We used a two-fingered gripper, while other alternative gripper types such as vacuum or humanoid hand grippers can be used. In addition, the gripper's maximum length of 15.2 cm is a critical factor for assessing accessibility as described in Figure 2.



Figure 2: Robotiq gripper connected with the UR5e.

The UR5e robotic arm conducts two main functions: positioning the gripper at designated locations and grasping objects. The performance of the grasping function is impacted by component size, weight, and shape, whereas the positioning function is determined by the factors of positioning and accessibility, as shown in Table 3. Each factor is assigned a median score of 3. The aggregate scores of 9 and 6 represent the sum of factors associated with robotic capability and can be benchmarked to distinguish between low and high capability levels.

Table 3: The relationship between factors of disassembly scores and robotic capability.

Factors	Robotic Capability	Scores
Component size		Low: ≤ 9
Component weight	Grasping	High: > 9
Component shape		
Positioning	D1:	Low: <= 6
Accessibility	Placing	High: > 6

2.1.3 The usage of disassembleability score

The robot's capability determines the work environment configurations, such as Human-Robot Collaboration (HRC), Semi-HRC, and Worker-Only settings, as shown in Figure 3. In an HRC setting, there is a collaboration between the human worker and the robotic arm, where humans and robots work on the same task. On the other hand, Semi-HRC shows a work setting where tasks between humans and robots are either sequential or parallel. The Worker-Only setting applies when the object's weight or size exceeds the robotic arm's capacity for manipulation and requires direct human intervention without the robot's assistance.

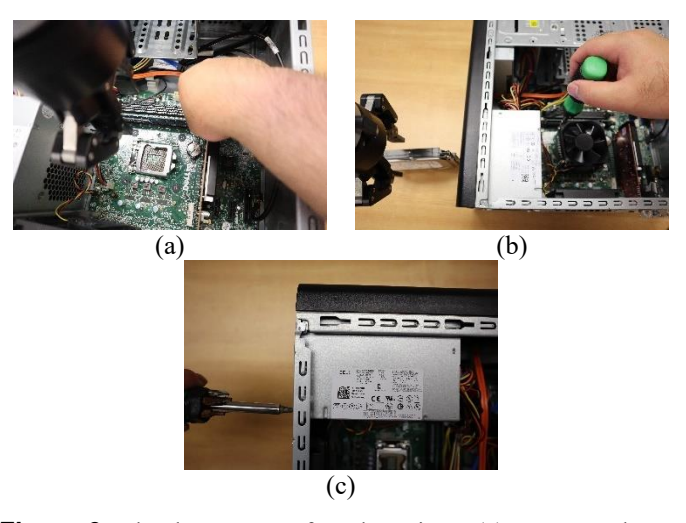


Figure 3: The three types of work settings: (a) Human-robot collaboration, (b) Semi-HRC, and (c) Worker only.

Figure 3 presents three scenarios: (a) HRC, (b) Semi-HRC, and (c) worker-only. In Figure 3(a), a human worker and a robot collaborate to disassemble a RAM module. The human releases the slot and holds the RAM, while the robot places and grabs it. Figure 3(b) depicts Semi-HRC, where the robot grabs the HDD, and the human worker unscrews the CPU fan bolts. The HDD placement follows a sequence where the human disassembles it before the robot intervenes. Figure 3(c) illustrates the worker-only disassembly of the power supply, as its size prevents the robot from handling it.

2.2 Applying MaxViT to classify component size

The MaxViT (Multi-Axis Vision Transformer) machine learning model is used to determine the size of components, which is a critical factor in disassembly processes. According to

[26], the MaxViT was introduced in 2022. This architecture combines the MaxViT block with MBConv (Mobile Inverted Bottleneck Convolution) [27], Block Attention, and Grid Attention mechanisms. MBConv combines the squeeze-and-excitation (SE) module with convolution layers to improve feature extraction. This research uses the MaxViT model to classify component sizes into four categories: small, medium, large, and oversized. The process consists of segmenting the input from an RGB image and categorizing it into one of these four size classes.

2.3 Human-robot collaborative disassembly time

In practical applications, it is important to note that the allocation of disassembly tasks between humans and robots should be determined not only based on their capabilities but also by considering the disassembly time required for each task. In this section, we introduce a general framework to calculate disassembly times for both manual operations and human-robot collaboration scenarios. We identify the optimal option as the minimum between the manual disassembly time and the human-robot collaboration disassembly time.

Human-robot collaborative disassembly time is derived from the operational time estimates from connector specifications by using disassembly parameters. We can use a user-friendly spreadsheet to calculate disassembly time. Within this spreadsheet, individual rows represent different connectors, and their arrangement determines the disassembly sequence under evaluation. The ease of disassembly time metric requires three parts: disassembly information, disassembly parameters, and individual humans' and robots' disassembly time (Figure 4).

Disassembly information consists of four segments, provided by product designers. First, the Product Description defines information about components and connectors. The subsequent Manual disassembly description provides details regarding connector visibility, tools required, positioning, manipulation techniques, and component removal procedures. The Robot disassembly factors evaluate the feasibility of robotic disassembly for connectors considering the five factors discussed in disassembly scores. Finally, the Robot disassembly description provides the specifics of robotic disassembly, including task types, tools employed, positioning considerations, fixture manipulation, grasping techniques, and methods for component removal.

Disassembly parameters consist of parameters that are used to calculate the disassembly time based on the provided disassembly information. It incorporates both calculated time parameters and robotic disassembly factor parameters. Manual disassembly time parameters are computed using the MOST technique [4] and the robotic disassembly time is calculated through experiments. For robotic disassembly parameters, the calculation incorporates a 50% maximum robot speed assumption based on a robot's maximum cartesian speed of 10 m/s, accounting for trapezoidal motion profiles and short distances during disassembly. Fixed action times of 5s are assumed for tool changing, grasping, and precise positioning and 2.5s seconds for task handover.

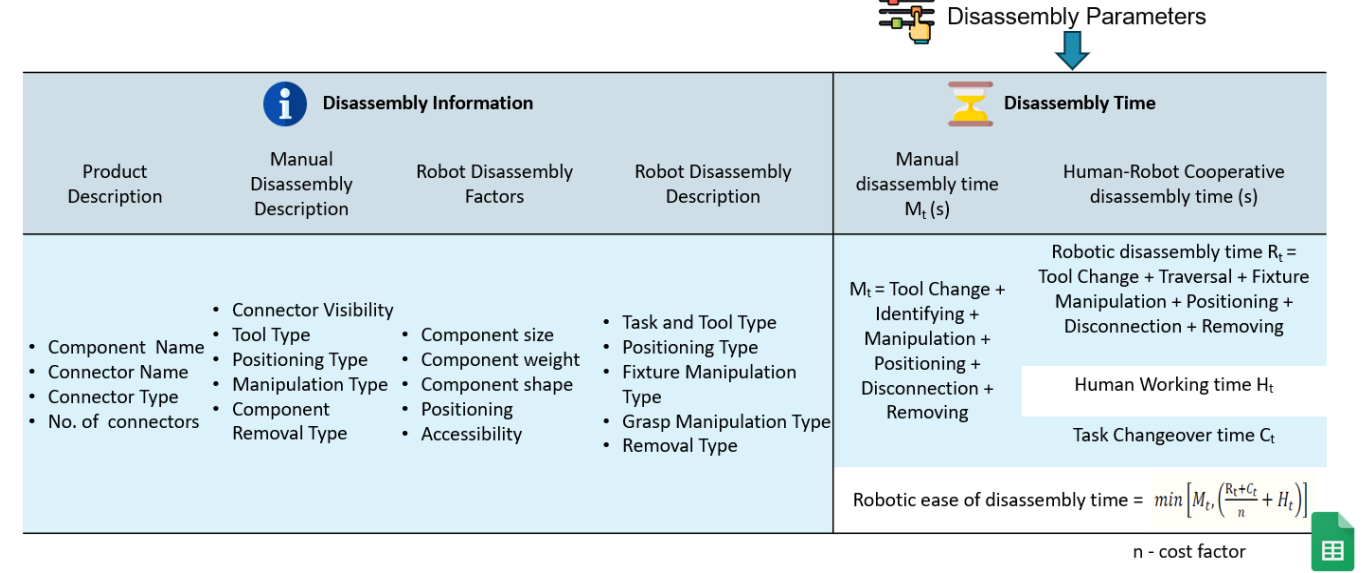


Figure 4: Human-robot collaborative disassembly time metric.

The parameters for the robotic disassembly factor take into account the disassembly scores. It is worth noting that disassembly parameters are calculated parameters, not measured parameters and as the robotic setup might vary for different applications, a generic robotic setup parameter is assumed for the metric which aids in evaluating the product design irrespective of the human-robot collaborative setup design. These parameters could be revised by the remanufacturers depending on their setup for obtaining a more accurate disassembly time for task planning and scheduling.

Now, to determine whether to select manual disassembly or HRC, we need to calculate Manual Disassembly Time (M_t) , and Human-Robot Collaborative Time. Manual Disassembly time (M_t) is calculated using:

$$M_t = Tool Change + Identifying + Manipulation + Positioning + Disconnection + Removing$$
 (2)

Human-Robot Collaborative Time is calculated using the following equation:

Human Robot collaboartive time =
$$\left(\frac{R_t + C_t}{n} + H_t\right)$$
 (3)

Where R_t is the Robotic disassembly time calculated using, $R_T = Tool \ change + Traversal$

- + Fixture Manipulation + Positioning
- + Disconnection + Removing

 C_t is the Task handover time which is determined by counting task transitions between humans and robots.

n is the cost factor and it is determined based on parameters such as robot usage cost, availability, and labor cost (e.g., n = 2, assuming the robot incurs half the labor cost).

If a task is executable by both a human and a robot, the metric attributes it to the robot, calculating the remaining tasks

as human working time (H_t). The final disassembly time is then computed as the minimum time between manual and human-robot collaborative disassembly.

3. CASE STUDY

3.1 XPS 8700 desktop

This study used an XPS 8700 desktop computer as a case study to show the application of the proposed disassembly score. Figure 5 and Table 4 show the images and the list of components, including the power supply, HDD, CD reader, and other electronic devices. The desktop has two memory RAMs that were disassembled. Figure 6 shows the precedence relationships among the components, where the number in each cycle corresponds to the entries in Table 4. The figure differentiates between two types of lines: those without arrows indicate components at the same level of disassembly sequence, whereas lines with arrows show that certain components should be removed before proceeding to the next component. We excluded the side cover and the base as they are too large for the robotic gripper's capacity.



Figure 5: The components of the XPS 8700 desktop.

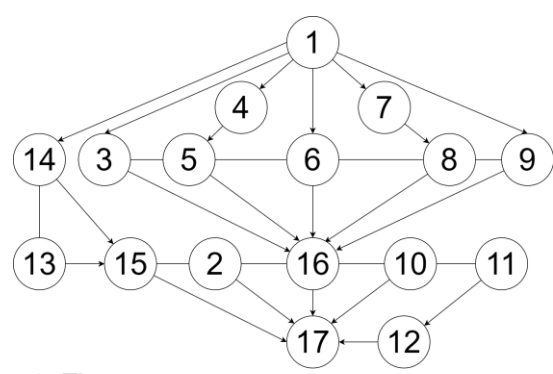


Figure 6: The precedence relationships of XPS 8700 disassembly tasks.

Table 4: The list of the components of XPS 8700.

#	Component	#	Component	#	Component
1	Side Cover	7	1st RAM	13	Front Cover
2	Port Cover	8	2nd RAM	14	Orange Cable
3	Side Fan	9	Power Supply	15	CD Reader
4	CPU Fan	10	HDD Cover	16	Motherboard
5	CPU Chip	11	Blue Cable	17	Base
6	GPU Card	12	HDD		

3.2 Components used for classification by MaxViT

Seven components were selected for analysis using the MaxViT model to identify component sizes. These components include a CD reader, HDD, CPU chip, GPU card, CPU fan, front cover, and power supply. Classification results show that the GPU card and HDD are considered small size; the CD reader and CPU chip are medium size; the CPU fan and front cover are large size; and the power supply is oversized. The camera was positioned at an equal distance for each component.

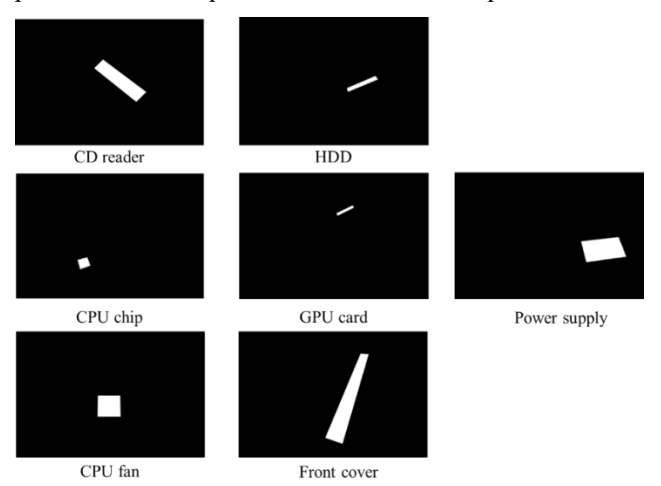


Figure 7: Segmented images of seven components: CD reader, HDD, CPU chip, GPU card, CPU fan, front cover, and power supply.

Moreover, we have collected 130 RGB images, which were manually labeled and resulted in 209 segmented images, as some examples are shown in Figure 7. These segmented images were divided into training, validation, and testing datasets, with a ratio

of 70%, 15%, and 15%, respectively. Data augmentation techniques were used on the training dataset before training the MaxViT model.

This study manually labels image segmentations, as shown in Figure 7, and uses these segmented images as inputs to the MaxVit model for classifying component sizes. Although manual segmentation requires extra preprocessing, it increases accuracy by creating precise boundaries, improving training data quality, and reducing background noise. This method also benchmarks automated segmentation, reduces overfitting, and is helpful for high-precision tasks such as medical imaging and component analysis. In practice, RGB images can be directly input into the classification model or first processed by a segmentation model to create segmented images for MaxVit to identify size classifications. While training a single object detection model may be simpler, a separate segmentation model offers valuable benefits despite the added complexity.

4. RESULTS AND DISCUSSIONS

This section presents the disassembly score calculated for the XPS 8700 desktop, along with the application of the MaxViT machine learning model for classifying component sizes and disassembly time calculation.

4.1 Disassembly score for the XPS 8700 desktop

The disassembly score is calculated for each component of the XPS 8700 desktop. Table 5 lists the characteristics of each component in terms of five factors: size, weight, shape, positioning, and accessibility. The shape of the component is quantified using Equation (1), while positioning shows the component's order of rotational symmetry. Based on the data in Table 5, Table 6 shows the corresponding score for each factor. Most of the components are small in size and lightweight. The CPU chip and CD reader are categorized as medium-sized, whereas the CPU fan and front cover are large. The power supply and motherboard are considered oversized, as their sizes exceed the maximum gripper opening of 8.5 cm. The blue and orange cables are considered asymmetric due to their variable shapes.

Regarding positioning, most components have an even order of rotational symmetry and are more accessible for the robot to handle. However, cables and the front cover are challenging to manipulate since their order of rotational symmetry is 1. Accessibility is limited for most components due to tight integration with the desktop casing or restricted space. The GPU card and two cables have medium accessibility, while the second RAM slot has sufficient space for the robotic gripper to navigate inside the desktop shell.

Table 7 shows the robotic capabilities for grabbing and placing components. The grabbing scores are calculated from the cumulative values of component size, weight, and shape, and the placing scores are calculated from the aggregation of positioning and accessibility. Due to oversized dimensions, the power supply and motherboard need manual disassembly. Most of the components have high grabbing capability due to their lightweight and favorable shape; however, they have low placing capability.

Table 5: The information of five factors for each component of the XPS 8700 desktop.

Component	Size (cm)	Weight (g) Shape (Ref. Symmetry)	Positioning (Rot. Symmetry)	Accessibility
Port Cover	8.8x0.4x1	15	1	2	No space
Side Fan	9.2x9.2x1.5	75	1	4	No space
CPU Fan	8x8x6	365	1	4	No space
CPU Chip	3.8x3.8x0.4	25	1	4	No space
GPU Card	5.5x9.6x1.5	140	1	2	Need to remove the CPU fan
1st RAM	3x13.5x0.1	10	1	2	Need to remove the GPU card and 1st RAM
2nd RAM	3x13.5x0.1	10	1	2	High Accessibility
Power Supply	14x15x8.6	1540	1	2	No space
HDD Cover	11x13.7x0.1	135	1	2	No space
Blue Cable	26.5x0.8x0.3	5	< 0.5	1	Medium Accessibility
HDD	11x14.6x2	390	1	2	No space
Front Cover	5x18x41	570	1	1	No space
Orange Cable	36.5x0.8x0.3	5	< 0.5	1	Medium Accessibility
CD Reader	14.6x17x4.1	645	1	2	No space
Motherboard	22.2x24x0.4	460	1	2	No space

Table 6: The resulting score for each factor.

Component	Size	Weight	Shape	Positioning	Accessibility
Port Cover	Small (1)	Light (5)	Symmetric (5)	Easy (5)	Low (1)
Side Fan	Small (1)	Light (5)	Symmetric (5)	Easy (5)	Low (1)
CPU Fan	Large (5)	Light (5)	Symmetric (5)	Easy (5)	Low (1)
CPU Chip	Medium (3)	Light (5)	Symmetric (5)	Easy (5)	Low (1)
GPU Card	Small (1)	Light (5)	Symmetric (5)	Easy (5)	Medium (3)
1st RAM	Small (1)	Light (5)	Symmetric (5)	Easy (5)	Low (1)
2nd RAM	Small (1)	Light (5)	Symmetric (5)	Easy (5)	High (5)
Power Supply	X	Light (5)	Symmetric (5)	Easy (5)	Low (1)
HDD Cover	Small (1)	Light (5)	Symmetric (5)	Easy (5)	Low (1)
Blue Cable	Small (1)	Light (5)	Asymmetric (1)	Difficult (1)	Medium (3)
HDD	Small (1)	Light (5)	Symmetric (5)	Easy (5)	Low (1)
Front Cover	Large (5)	Light (5)	Symmetric (5)	Difficult (1)	Low (1)
Orange Cable	Small (1)	Light (5)	Asymmetric (1)	Difficult (1)	Medium (3)
CD Reader	Medium (3)	Light (5)	Symmetric (5)	Easy (5)	Low (1)
Motherboard	X	Light (5)	Symmetric (5)	Easy (5)	Low (1)

Table 7: The work settings based on disassembly factors and robotic capability.

Component	Grasping	Placing	Grasping Capability	Placing Capability	Work Setting
Port Cover	11	6	High	Low	Semi-HRC
Side Fan	11	6	High	Low	Semi-HRC
CPU Fan	15	6	High	Low	Semi-HRC
CPU Chip	13	6	High	Low	Semi-HRC
GPU Card	11	8	High	High	HRC
1st RAM	11	6	High	Low	Semi-HRC
2nd RAM	11	10	High	High	HRC
Power Supply	X	X	X	X	Human worker only
HDD Cover	11	6	High	Low	Semi-HRC
Blue Cable	7	4	Low	Low	Human worker only
HDD	11	6	High	Low	Semi-HRC
Front Cover	15	2	High	Low	Semi-HRC
Orange Cable	7	4	Low	Low	Human worker only
CD Reader	13	6	High	Low	Semi-HRC
Motherboard	X	X	X	X	Human worker only

This limitation in placing capability is because of the limited space available, as listed in Tables 5 and 6, which results in most of the components being classified under semi-HRC conditions. This classification means the worker should position the component precisely before the robot grabs it and places it into the collection bin. The GPU card and second RAM have a high capability for both grabbing and placing, where the robotic gripper can access and manipulate these components inside the desktop. The robotic arm can work with the worker concurrently under the HRC setting.

4.2. Component size classification results

This limitation in placing capability is because of the limited space available, as listed in Tables 5 and 6, which results in most of the components being classified under semi-HRC conditions. This classification means the worker should position the component precisely before the robot grabs it and places it into the collection bin. The GPU card and second RAM have a high capability for both grabbing and placing, where the robotic gripper can access and manipulate these components inside the desktop. The robotic arm can work with the worker concurrently under the HRC setting.

The MaxViT classifies component sizes into four categories: small, medium, large, and oversize, which are assigned labels 1, 2, 3, and 4, respectively.

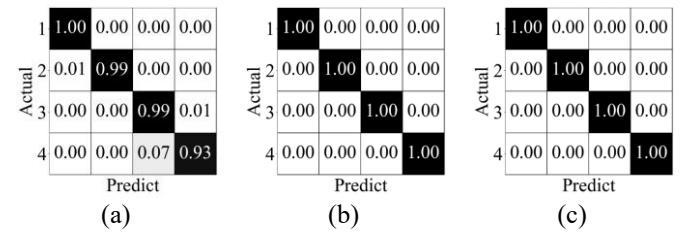


Figure 8: The normalized confusion matrix of (a) training results with 98% accuracy, (b) validation results with 100% accuracy, and (c) testing results with 100% accuracy.

Figure 8 shows the normalized confusion matrix results of training, validation, and testing datasets. The training accuracy is 98%, while the validation and testing accuracy is 100%. The MaxViT model can classify the component size perfectly. In the training phase shown in Figure 8 (a), the sizes, such as medium, large, and oversize, lost some accuracy, which the MaxViT classed into the nearby size. For example, in oversize (4), 7% of images are classed into large sizes, and others, such as small and medium, do not have misclassification. This shows the capabilities of using machine learning to identify disassembly factors towards an automated rating system.

In this study, we do not consider summing the pixels in segments. While summing pixels can indicate the area of a component, it does not reflect whether the robot can grasp it. For instance, two objects- one measuring 90x90 mm and another 30x270 mm- have the same area, but the robot cannot grasp the first one due to its 85 mm limitation.

The MaxViT model demonstrates an example of classification with automated size assessment. This example

suggests that future studies could develop an automated rating system for disassembly scores based on the MaxViT model, even with unknown size information. The deep learning model requires only the image as input and then evaluates the disassembly scores automatically.

4.3 Calculation of disassembly time for the XPS 8700 desktop

Considering the robot's capabilities and the design of the case study product especially low placing capability due to the limited space available, predominant of the tasks are carried out by manual disassembly. Considering the human-robot collaborative disassembly time calculation, the total manual disassembly time (M_t) for the XPS 8700 desktop was found to be 145.8 sec. Factoring in robotic capabilities, the robotic disassembly time (R_t) was 60.82 sec with the remaining tasks accounting for human working time (H_t) at 128.16 seconds and a task changeover time (Ct) of 37.5 seconds. Considering a cost factor (n) of 2, the final disassembly time was calculated as 145.8 seconds. We should note that the obtained disassembly time is based on the calculated disassembly parameters for uniformity of the product design evaluation and hence, the calculated disassembly time values will differ from the actual measured disassembly times in practice.

While the disassembly scores define each component's work setting, the disassembly time reflects the overall efficiency of the XPS 8700 desktop. This metric can inform product design improvements for more HRC-friendly disassembly. Future research can use disassembly time to evaluate different design alternatives.

5. CONCLUSION

This study proposes a framework for assessing the disassembly score suitable for robotic disassembly based on five factors: component size, weight, shape, positioning, and accessibility. It discusses the connection between disassembly factors, robotic capabilities, and workplace settings. The application of the proposed disassembly score is shown by using an XPS 8700 desktop. Moreover, the study uses MaxViT, a transformer-based machine learning model, to categorize component sizes into four classes: small, medium, large, and oversized. The framework provides a rating system for determining the ease of robots performing disassembly tasks. Further, the use of MaxViT proves that artificial intelligence techniques can be used to automate the development of scoring systems. The study also provided a framework for comparing manual disassembly time with human-robot disassembly time as the base for decision-making and determining a practical disassembly work setting.

The study can be extended in several ways. The future automated rating systems can be further developed. It will be easier for robots to evaluate the ease of disassembly and handling of each component by using computer vision techniques. Moreover, other types of robotic grippers, such as vacuum and humanoid hand grippers, can be used beyond just the two-finger gripper. The analysis mainly considers the robotic perspective

and neglects the human worker's viewpoint. Future research could broaden the disassembly scoring framework to include both robotic and human considerations, such as human factors and fatigue. Also, the use of a disassembly score can be shown in the product design phase to facilitate designing products that are easier for robots to disassemble.

ACKNOWLEDGEMENT

This material is based upon work supported by the National Science Foundation—USA under grant # 2026276. Any opinions, findings, conclusions, or recommendations expressed in this material are those of the authors and do not necessarily reflect the views of the National Science Foundation.

REFERENCES

- [1] S. Hjorth and D. Chrysostomou, "Human–robot collaboration in industrial environments: A literature review on non-destructive disassembly," *Robot Comput Integr Manuf*, vol. 73, p. 102208, 2022.
- [2] H. Liao, Y. Chen, B. Hu, and S. Behdad, "Optimization-Based Disassembly Sequence Planning Under Uncertainty for Human-Robot Collaboration." Jun. 27, 2022. doi: 10.1115/MSEC2022-85383.
- [3] A. Desai and A. Mital, "Evaluation of disassemblability to enable design for disassembly in mass production," *Int J Ind Ergon*, vol. 32, no. 4, pp. 265–281, 2003.
- [4] P. Vanegas *et al.*, "Ease of disassembly of products to support circular economy strategies," *Resour Conserv Recycl*, vol. 135, pp. 323–334, 2018.
- [5] IFixit, "Smartphone Repairability Scores." [Online]. Available: https://www.ifixit.com/smartphone-repairability
- [6] E. Bracquené *et al.*, "Analysis of evaluation systems for product repairability: A case study for washing machines," *J Clean Prod*, vol. 281, 2021, doi: 10.1016/j.jclepro.2020.125122.
- [7] M. Basiony, "Computerized equipment management system," *J Clin Eng*, vol. 38, no. 4, pp. 178–184, 2013, doi: 10.1097/JCE.0b013e3182a904e4.
- [8] F. De Fazio, C. Bakker, B. Flipsen, and R. Balkenende, "The Disassembly Map: A new method to enhance design for product repairability," *J Clean Prod*, vol. 320, p. 128552, 2021.
- [9] L. Qiu, X. Liu, S. Zhang, and L. Sun, "Disassemblability modeling technology of configurable product based on disassembly constraint relation weighted design structure matrix (DSM)," *Chinese Journal of Mechanical Engineering*, vol. 27, no. 3, pp. 511–519, 2014.
- [10] D. P. Yadav, D. N. Patel, and B. W. Morkos, "Development of product recyclability index utilizing design for assembly and disassembly principles," *J Manuf Sci Eng*, vol. 140, no. 3, p. 031015, 2018.
- [11] E. Bracquené *et al.*, "Analysis of evaluation systems for product repairability: A case study for washing

- machines," *J Clean Prod*, vol. 281, 2021, doi: 10.1016/j.jclepro.2020.125122.
- [12] G. Mummolo *et al.*, "a Fuzzy Approach for Medical Equipment Replacement Planning," *Third International Conference on Maintenance and Facility Management*, pp. 229–235, 2007.
- [13] J. R. Peeters, P. Tecchio, F. Ardente, P. Vanegas, D. Coughlan, and J. R. Duflou, eDIM: further development of the method to assess the ease of disassembly and reassembly of products Application to notebook computers. 2018. doi: 10.2760/864982.
- [14] W. Zhu, X. Fan, and Q. He, "A hierarchical and process-oriented framework for disassemblability evaluation in product maintainability design," *The International Journal of Advanced Manufacturing Technology*, vol. 110, pp. 777–795, 2020.
- [15] M. Germani, M. Mandolini, M. Marconi, and M. Rossi, "An approach to analytically evaluate the product disassemblability during the design process," *Procedia CIRP*, vol. 21, pp. 336–341, 2014.
- [16] H. Sawanishi, K. Torihara, and N. Mishima, "A study on disassemblability and feasibility of component reuse of mobile phones," *Procedia CIRP*, vol. 26, pp. 740–745, 2015.
- [17] A. Ali, C. Enyoghasi, and F. Badurdeen, "A quantitative approach for product disassemblability assessment," *Role of Circular Economy in Resource Sustainability*, pp. 73–84, 2022.
- [18] S. Parsa and M. Saadat, "Intelligent selective disassembly planning based on disassemblability characteristics of product components," *The International Journal of Advanced Manufacturing Technology*, vol. 104, no. 5, pp. 1769–1783, 2019, doi: 10.1007/s00170-019-03857-1.
- [19] T. F. Go, D. A. Wahab, M. N. A. Rahman, R. Ramli, and C. H. Azhari, "Disassemblability of end-of-life vehicle: a critical review of evaluation methods," *J Clean Prod*, vol. 19, no. 13, pp. 1536–1546, 2011.
- [20] N. Boix Rodríguez and C. Favi, "Disassembly and repairability of mechatronic products: insight for engineering design," *Journal of Mechanical Design*, vol. 146, no. 2, 2024.
- [21] K. Li, Q. Liu, W. Xu, J. Liu, Z. Zhou, and H. Feng, "Sequence planning considering human fatigue for human-robot collaboration in disassembly," *Procedia CIRP*, vol. 83, pp. 95–104, 2019.
- [22] S. Vongbunyong, S. Kara, and M. Pagnucco, "Basic behaviour control of the vision-based cognitive robotic disassembly automation," *Assembly Automation*, 2013.
- [23] S. Parsa and M. Saadat, "Human-robot collaboration disassembly planning for end-of-life product disassembly process," *Robot Comput Integr Manuf*, vol. 71, p. 102170, 2021.
- [24] H. Hu, Y. Liu, W. F. Lu, and X. Guo, "A quantitative aesthetic measurement method for product appearance

- design," *Advanced Engineering Informatics*, vol. 53, p. 101644, 2022.
- [25] P. Steinhardt, *The second kind of impossible: the extraordinary quest for a new form of matter.* Simon and Schuster, 2019.
- [26] Z. Tu *et al.*, "Maxvit: Multi-axis vision transformer," in *European conference on computer vision*, Springer, 2022, pp. 459–479.
- [27] M. Sandler, A. Howard, M. Zhu, A. Zhmoginov, and L.-C. Chen, "Mobilenetv2: Inverted residuals and linear bottlenecks," in *Proceedings of the IEEE conference on computer vision and pattern recognition*, 2018, pp. 4510–4520.